Asian Journal of Pharmaceutical Sciences 15 (2020) 83–94

Available online at www.sciencedirect.com

ScienceDirect

journal homepage: www.elsevier.com/locate/AJPS

Original Research Paper

Redox-responsive biocompatible nanocarriers based on novel heparosan polysaccharides for intracellular anticancer drug delivery

Lipeng Qiu[a,1], *Lu Ge*[a,1], *Miaomiao Long*[b], *Jing Mao*[a], *Kamel S. Ahmed*[a], *Xiaotian Shan*[a], *Huijie Zhang*[a], *Li Qin*[a], *Guozhong Lv*[c], *Jinghua Chen*[a,*]

[a] *School of Pharmaceutical Sciences, Jiangnan University, Wuxi 214122, China*
[b] *Wuxi Higher Health Vocational Technology School, Wuxi 214028, China*
[c] *Wuxi Third Renmin Hospital, Wuxi 214041, China*

ARTICLE INFO

Article history:
Received 5 July 2018
Revised 31 October 2018
Accepted 16 November 2018
Available online 17 December 2018

Keywords:
Heparosan
Vitamin E succinate
Redox-sensitive micelles
Drug delivery

ABSTRACT

Heparosan is a natural precursor of heparin biosynthesis in mammals. It is stable in blood circulation but can be degraded in lysosomes, showing good biocompatibility and long circulation features. So heparosan can be designed as anticancer drug carriers to increase tumor selectivity and improve the therapeutic effect. A novel redox-sensitive heparosan-cystamine-vitamin E succinate (KSV) micelle system was constructed for intracellular delivery of doxorubicin (DOX). Simultaneously, the redox-insensitive heparosan-adipic acid dihydrazide-vitamin E succinate copolymer (KV) was synthesized as control. DOX-loaded micelles (DOX/KSV) with an average particle size of 90–120 nm had good serum stability and redox-triggered depolymerization. *In vitro* drug release test showed that DOX/KSV micelles presented obvious redox-triggered release behavior compared with DOX/KV. Cytotoxicity and cell uptake were investigated using MGC80-3 tumor cells and COS7 fibroblast-like cells. The cell survival rate of blank micelles was more than 90%, and the cytotoxicity of DOX/KSV in MGC80-3 cells was higher than in COS7 cells, indicating that the carrier has better biocompatibility and less toxicity side effect. The cytotoxicity of DOX/KSV against MGC80-3 cells was significantly greater than that of free DOX and DOX/KV. Furthermore, compared with DOX/KV in MGC80-3 cells, DOX/KSV micelles uptook more anticancer drugs and then released DOX faster into the cell nucleus. The micelles were endocytosed by multiple pathways, but clathrin-mediated endocytosis was the main pathway. Therefore, heparosan polysaccharide could be a potential option as anticancer carrier for enhancing efficacy and mitigating toxicity.

* Corresponding author. Jiangnan University, No. 1800 Lihu Road, Wuxi 214122, China. Tel.: +86 510 85329042.
E-mail address: chenjinghua@jiangnan.edu.cn (J.H. Chen).
[1] These authors contributed equally to this work.
Peer review under responsibility of Shenyang Pharmaceutical University.

https://doi.org/10.1016/j.ajps.2018.11.005

1. Introduction

Cancer is a global public health problem. In the current treatment of cancer, chemotherapy is one of the most important methods [1]. Doxorubicin (DOX), an antibiotic anticancer drug, is used for multiple cancers such as bladder cancer, breast cancer, stomach cancer, ovarian cancer, thyroid cancer, lung cancer, multiple myeloma and soft tissue sarcoma [2–4]. However, the poor targeting and serious side effects limit the application of DOX [5–7]. In order to solve these problems, in the past several decades, drug delivery systems (DDS) have been developed for the delivery of DOX, such as liposomes, nanoparticles, and polymer micelles [8–10]. Among them, polymer micelles which are easy to prepare and applicable to all hydrophobic drugs have attracted attention due to their unique advantages. Polymer micelles are usually composed of hydrophobic core in which hydrophobic drugs can be loaded and hydrophilic shell which can keep the core away from the aqueous environment [11]. What's more, the structure can greatly increase the solubility and stability of hydrophobic drugs in aqueous solution, resulting in enhancing their bioavailability and blood circulation time. And the hydrophilic shell can protect the carrier from reticulo-endothelial system (RES) [12–18]. Polymer micelles also can improve the selectivity of tumor tissue through enhanced permeability and retention (EPR) effects to significantly increase the efficiency of anticancer drugs [6,19].

The materials for constructing polymer micelle can be divided into natural polymers and synthetic polymers according to their sources. Polyethylene glycol (PEG) is a commonly used synthetic material. PEGylated polymer micelles are widely used because of their prone to self-assembly, small particle size, narrow size distribution and unique shell and shell structure [20,21]. However, as the synthetic material, PEG has poor biodegradability and biocompatibility. PEG is metabolized to some accumulated toxic metabolites *in vivo*. Besides, studies have found that PEG shell can hinder the disassembly of the micelles and reduce drug release from tumor cells [22,23]. Natural materials have gradually become hotspot polymers to study due to their high biocompatibility and biodegradability. The natural polymer materials are represented by polysaccharides such as chitosan [24], hyaluronic acid [25] and heparin [26]. However, most of polysaccharides can be degraded by enzyme resulting in short circulation time of nanoparticles *in vivo*. Therefore, how to design a better delivery system becomes an important issue. Heparosan (HR) is a natural precursor to heparin biosynthesis in mammals and a heparin-like material. But unlike heparin, HR will not be degraded by heparanase *in vivo* because of the unsulfated oxygen site, which endows HR with long circulation effect. However, HR can be degraded by glucuronidase and hexosaminidase to N-acetylglucosamine and glucuronic acid in lysosomes. The degradation products are normal monosaccharides *in vivo* and can be recycled by cells without accumulation in the tissue [27]. Therefore, HR has good biocompatibility and HR-based drug delivery systems are considered "zero-residue" system [28].

After arrival at tumor cell, anticancer drugs encapsulated into the polymer micelles need to be released in time to achieve their high therapeutic efficiency for tumors [29,30]. Some studies also have shown that faster intracellular drug release can improve cytotoxicity and overcome MDR [31]. In recent years, environmental stimuli-responsive polymer micelles have been widely used for delivery and controlled release of anticancer drugs. Stimuli-responsive polymer micelles can be triggered by pH, temperature, enzymes, redox potentials, light, magnetic fields and ultrasound waves [32–38] to rapidly release the loaded drugs. Among them, redox-sensitive polymer micelles have been widely studied because of the difference redox content between extracellular and tumor cells [39–41]. It is noteworthy that many tumor cells have higher glutathione (GSH) concentrations than normal cells [42]. This difference can cause rapid release of active ingredients such as drugs, genes, and proteins from the redox-sensitive carriers resulting in a stronger therapeutic effect [43–45].

In this study, high-purity HR polysaccharide obtained by a combination of modern separation and chromatography techniques was used to prepare the redox-sensitive amphiphilic copolymer. Vitamin E succinate was linked to polysaccharide by cystatines (CYS) to synthesize heparosan-cystamine- vitamin E succinate (KSV) copolymers. And redox-insensitive heparosan-adipic acid dihydrazide-vitamin E succinate (KV) copolymers were synthesized as controls. Using DOX as a model anticancer drug, the properties of blank micelles and drug-loaded micelles were investigated. The cytotoxicity and intracellular release of the micelles against MGC80-3 cells and COS7 cells were evaluated. Furthermore, the internalization pathways of DOX-loaded micelles were further tested. The preparation and antitumor effect of DOX-loaded micelles is shown in Scheme 1.

2. Materials and methods

2.1. Materials

Heparosan was separated and purified in the lab. D-α-tocopherol acid succinate (VES), N-hydroxysuccinimide (NHS) and 1-ethyl-3-(3-dimethylaminopropyl) carbodiimide (EDC) were purchased from Aladdin Regent Co. (Shanghai, China). Adipodihydrazide (ADH), cystamine dihydrochloride (CYS) were provided by Energy Chemical Reagent Co. Ltd (Shanghai, China). Dimethyl sulfoxide (DSMO), dithiothreitol (DTT), pancreatin and penicillin-streptomycin solution were obtained from Shanghai Songan Biotech Co. Ltd (Shanghai, China). Tetrahydrofuran (THF), dimethylformamide (DMF), formamid and triethylamine (TEA) were obtained from Shanghai Reagent Chemical Co. Ltd (Shanghai, China). Doxorubicin hydrochloride (DOX•HCl) was purchased from Dalian Meilune Biotech Co. Ltd (Dalian, China). Fetal bovine serum (FBS), Dulbecco's modified eagle medium (DMEM) and RPMI-1640 medium were purchased from Gibco BRL (Maryland, USA). 3-[4,5-*dimethylthiazol*-2-*yl*]−2,5-diphenyltetrazoliumbromide (MTT) was obtained from Invitrogen Corp. 4,6-diamidino-2-phenylindole (DAPI) were obtained from Shanghai Beyotime Biotechnology Co. Ltd. (Shanghai, China). All other reagents were of analytical grade.

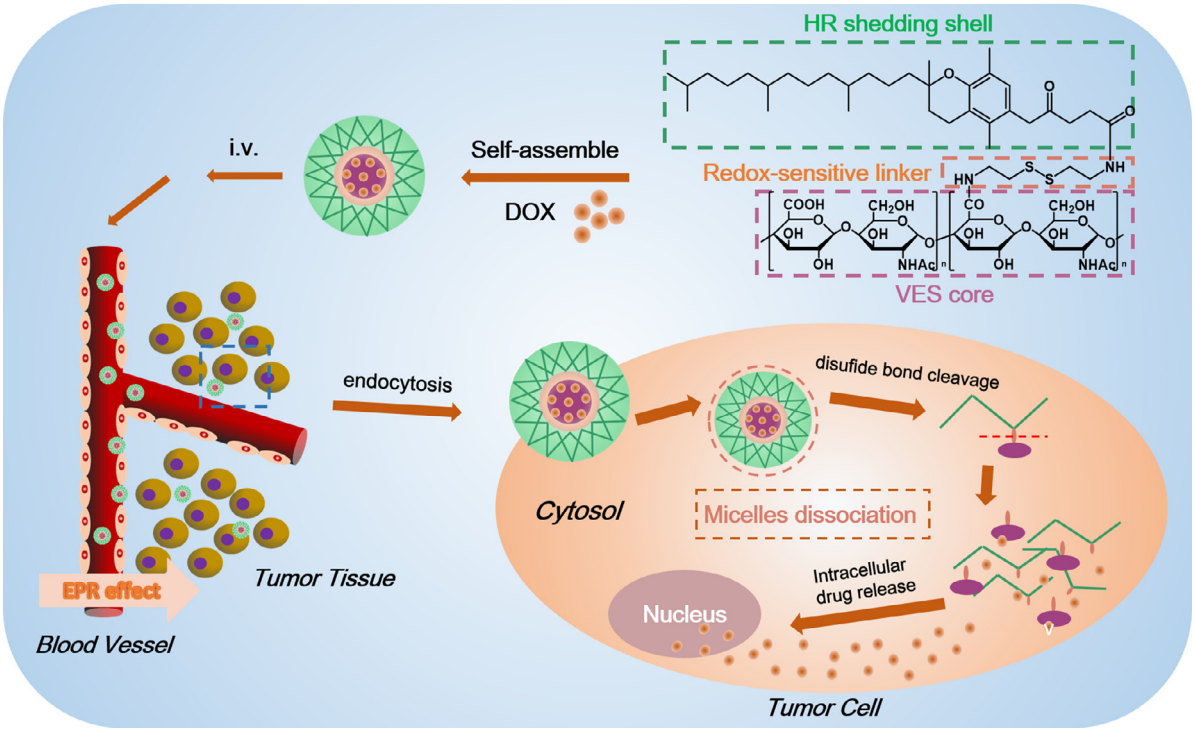

Scheme 1 – The preparation and antitumor effect of redox-responsive DOX/KSV micelles.

2.2. *Cell culture*

Human gastric cancer cells (MGC80-3) and transformed African green monkey SV40-transformed kidney fibroblast cells (COS7) were purchased from Chinese Academy of Sciences (Shanghai, China) and grown in DMEM (Gibco, USA) supplemented with 10% fetal bovine serum (FBS), 100 mg/ml streptomycin sulfate, 100 U/ml penicillin G sodium. Cells were incubated at 37 °C in a humidified atmosphere containing 5% CO_2.

2.3. *Synthesis of redox-sensitive KSV copolymers*

Cystamine-vitamin E succinate was prepared firstly. Cystamine dihydrochloride was pretreated by NaOH solution through acid-base neutralization [46]. Vitamin E succinate (1.5×10^{-4} mol) was dissolved in DMF at room temperature and EDC (3×10^{-4} mol) and NHS (3×10^{-4} mol) were added to the solution successively to activate carboxylic groups. Cystamine (1.5×10^{-4} mol, 1:1; 7.5×10^{-4} mol, 5:1) dissolved in DMF (5 ml) and was dropped into the vitamin E succinate solution, stirring for 48 h under a nitrogen atmosphere at room temperature. After completion, the solution was dialyzed in the dialysis bag (MWCO 3500) against distilled water for 2 d, and then freeze-dried to obtain cystamine-vitamin E succinate.

Then heparosan (1.5×10^{-4} mol) was dissolved in formamide. After activation of the carboxyl groups, heparosan was dropped into the cystamine-vitamin E succinate (1.5×10^{-4} mol) solution and then stirred for 48 h under a nitrogen atmosphere at room temperature. After the reaction finished, the mixture was allowed to dialyze in the dialysis membrane (MWCO 3500) against 25% ethanol solution and pure water, and then freeze-dried to obtain KSV copolymers.

2.4. *Synthesis of redox-insensitive KV copolymers*

As controls, the insensitive KV copolymers were also synthesized by two steps. Firstly, adipic acid dihydrazide (7.25×10^{-4} mol) and EDC (2.5×10^{-4} mol) were added into the heparosan (1.25×10^{-4} mol) solution. The pH of mixture solution was adjusted to 4.75 by 0.1 M HCl and stirred for 1 h. Then the reaction was ended by the addition of 0.1 M NaOH. The solution was dialyzed (MWCO 3500) in distilled water for 2 d, and freeze-dried to obtain Heparosan-ADH.

Secondly, VES (1.5×10^{-4} mol) was dissolved in a mixed solution of dimethylformamide and formamide and activated by EDC and NHS. Heparosan-ADH (1.5×10^{-4} mol) was dropped into the VES solution and stirred for 48 h under a nitrogen atmosphere at room temperature. The reaction solution was allowed to dialyze in the dialysis membrane (MWCO 3500) against 0.1 M sodium chloride, 25% ethanol solution, and pure water, and finally freeze-dried to obtain KV copolymers.

2.5. *Preparation of DOX-loaded micelles*

DOX•HCl (10 mg, 0.017 mmol) was dissolved in methanol (10 ml). After adding triethylamine (1 ml), the solution was stirred at room temperature for 24 h. The organic solvent was removed by rotary evaporation, and then tetrahydrofuran was added to obtain DOX base form solution. KSV copolymer (10 mg) was dissolved in PBS (pH 7.4, 10 ml). After sufficient dispersion, the DOX base form solution (2 ml) was slowly dropped into the solution and the mixture solution was

stirred overnight in dark. DOX-loaded KSV polymer micelles (DOX/KSV) were got after ultrasonic 30 min in an ice bath. Similarly, DOX-loaded KV polymer micelles (DOX/KV) were also prepared with the similar method.

2.6. Characterization of the micelles

The average particle size, distribution and zeta potential of the micelles were investigated by Zetasizer Nano ZS apparatus (MalvernInstruments, UK) at 37 °C. The morphology of DOX/KSV and DOX/KV micelles were observed by JEM-2100 TEM with acceleration voltage was 80 kV (JEO, Japan). Typically, the micelles were dropped onto the copper grid and the solution was evaporated. Then it was negatively stained with 2% phosphotungstic acid before observation.

The critical micelle concentration (CMC) of KSV and KV copolymers was determined by fluorescence spectrophotometer (RF-5301 PC, Shimadzu, Japan) with pyrene as a hydrophobic probe [47]. Briefly, after pyrene solution completely evaporated under a nitrogen stream, a series of polymer solutions with a concentration of 1.0×10^{-4} to 2.0 mg/ml were added to the tubes to obtain a final pyrene concentration of 6.0×10^{-7} M. The excitation spectrum of pyrene was determined by fluorescence spectrophotometer, and CMC value was calculated according to the change of the excitation spectrum.

2.7. Serum stability and redox-triggered disassembly of micelles

The serum stability and redox-sensitive test of the polymer micelles were measured by dynamic light scattering spectrophotometry (Zetasizer Nano ZS apparatus, MalvernInstruments, UK), as described by Choi et al. with some modification [48]. Briefly, the micelles were dissolved in pH 7.4 PBS solution mixed with DMEM solution containing 10% FBS, and the changes of size were measured at different times. In order to verify the reduction-sensitive of KSV copolymers, the micelles were dispersed in GSH-containing PBS solution (10 mM, pH 7.4) and tested at programmed times.

2.8. Determination of drug-loading efficiency

In order to detect the contained drugs, free DOX was separated by ultrafiltration firstly. Dimethyl sulfoxide was added into the micelles to destroy the micellar structure. According to this method, encapsulation efficiency (EE) and drug loading content (DL) were tested by an UV spectrophotometer (UV-2550, Shimadzu, Japan) with wavelength of 480 nm.

2.9. In vitro reduction-triggered release behaviors

The release of DOX from the both micelles *in vitro* was tested using dialysis method. The drug-loaded micelles were placed into the dialysis bags (MWCO 1000) which were immersed in 20 ml of different medium at 37 °C, 100 r/min conditions. At a predetermined time point, the medium was sampled to calculate the cumulative release of DOX as follows:

$$\mathrm{Er}\,\% = \frac{V_e \sum_{1}^{n-1} C_i + V_0 C_n}{m_{DOX}} \times 100$$

Where, *Er* represents the cumulative release of DOX, m_{DOX} is the content of the drug in the micelles, V_0 represents the total volume of the release medium, V_e is the replacement volume of the release medium and C_i represents the drug concentration released at the i^{th} sample.

2.10. In vitro cytotoxicity assays

The *in vitro* cytotoxicity of blank micelles and drug-loaded micelles was determined by MTT assay using cancer cells (MGC80-3) and normal cells (COS7). Briefly, COS7 and MGC80-3 cells were seeded in 96-well plates at a density of 5×10^3. After incubated for 24 h, the prepared blank micelles with a concentration range of 0–500 μg/ml and drug-loaded micelles with a concentration range of 0–10 μg/ml (DOX/KV, DOX/KSV) were added to replace the old medium. Then, 100 μl MTT solution was added to each well and incubated for 4 h. MTT solution was discarded and DMSO (100 μl) was added to dissolve blue-violet crystals. The absorbance at 570 nm was measured by using Multiskan MK3 microplate reader (Thermo, USA) to calculate the cell viability. The IC_{50} values were calculated using SPSS 17.0 (Chicago, IL, USA).

2.11. Observation of the cellular uptake of DOX-loaded micelles

The intracellular distribution of free DOX, DOX/KSV and DOX/KV micelles in MGC80-3 and COS7 cells were observed by confocal laser scanning microscopy (CLSM, Nikon A1R, Japan). MGC80-3 and COS7 cells were seeded into a laser confocal dish at a density of 1.5×10^5 cells/well. Free DOX or drug-loaded micelles (DOX conc entration of 5.0 μg/ml) were added and after 1 h, 2 h and 4 h of incubation, the cells were fixed by 4% paraformaldehyde solution. Then, DAPI fluorescent dye (20 μg/ml, 30 min) was used to make the nucleus visible. The remaining DAPI fluorescent dye was thoroughly washed with PBS, and 300 μl of PBS was added to each well for observation by CLSM.

2.12. Flow cytometry analysis

The cellular uptakes of free DOX, DOX/KSV and DOX/KV micelles in MGC80-3 and COS7 cells were measured by flow cytometry (FCM) (BD FACSCalibur). The cells were plated in 6-well plates at a density of 4×10^5 cells/well. After Incubated at 37 °C and 5% CO_2 for 12 h, the medium was replaced with free DOX or drug-loaded micelles (DOX concentration of 5.0 μg/ml). After incubated for different times, the cells were dispersed into PBS and measured by FCM.

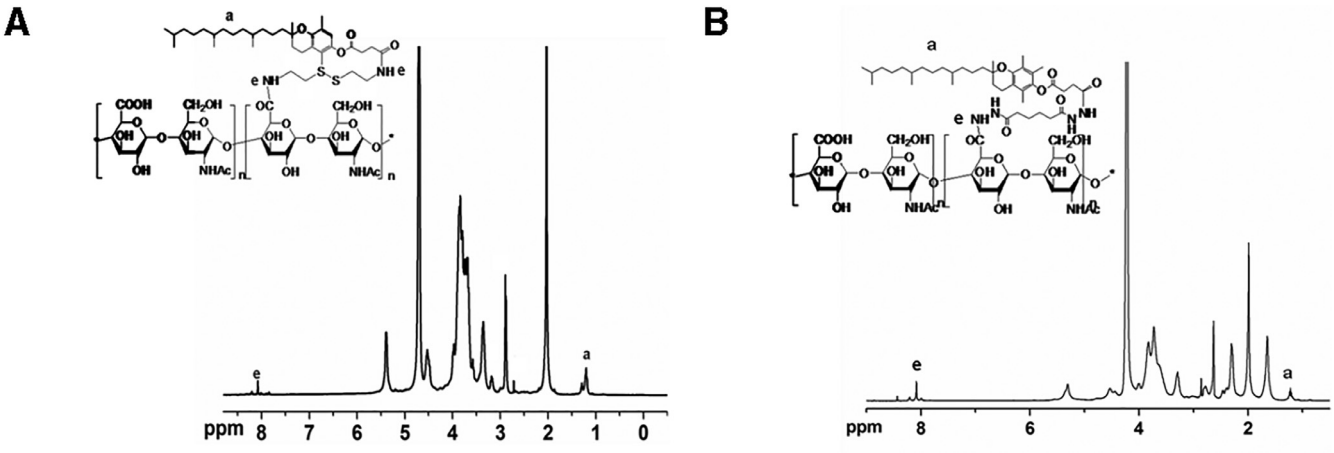

Fig. 1 – ^{1}H NMR spectra of KSV (A) and KV (B) copolymers.

Table 1 – Characterization of blank micelles and drug-loaded micelles.

	Micelles sizes (nm)	PDI	Zeta potential (mV)	DL (%)	EE (%)	CMC (mg/l)
KSV_{17}	102.4 ± 5.7	0.157 ± 0.01	−23.9 ± 3.3	–	–	18.47 ± 2.51
KSV_{21}	99.6 ± 4.6	0.128 ± 0.01	−22.6 ± 2.5	–	–	16.53 ± 3.26
DOX/ KSV_{17}	131.6 ± 3.9	0.137 ± 0.01	−20.5 ± 4.2	88.92 ± 5.22	13.28 ± 1.56	
DOX/ KSV_{21}	126.0 ± 5.2	0.147 ± 0.01	−19.7 ± 2.1	90.71 ± 2.70	15.37 ± 1.69	

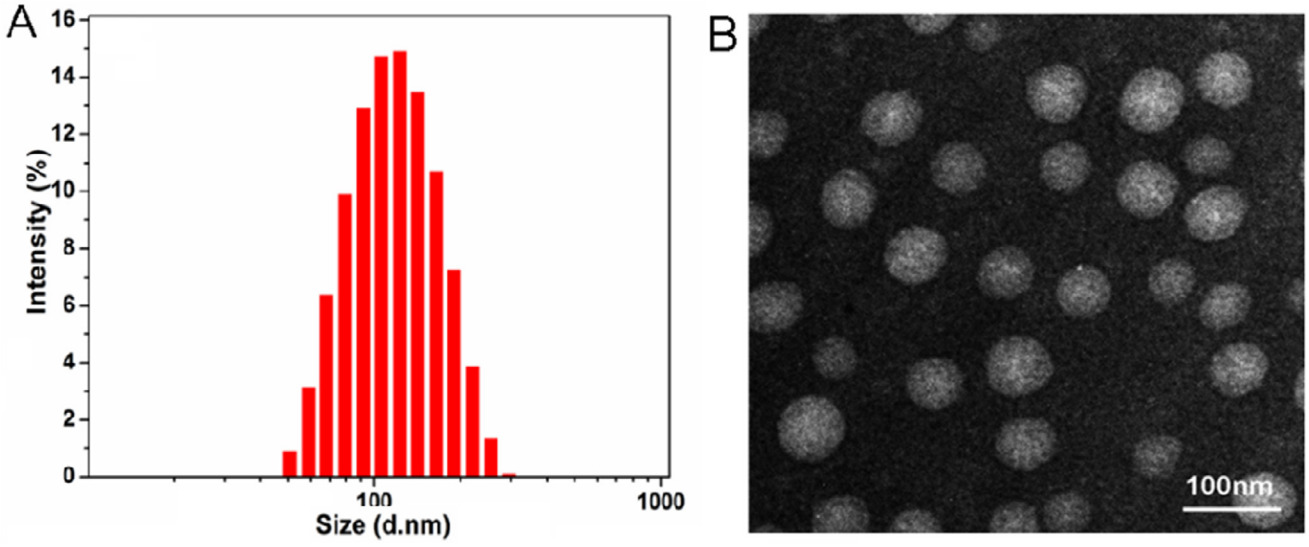

Fig. 2 – (A) Particle size of DOX/KSV in 10% PBS at 37 °C determined by DLS at defined time points. (B) TEM image of DOX/KSV. Scale bars correspond to 100 nm in the image.

2.13. *Study of the cellular uptake mechanism*

2.13.1. *Effects of ATP depletion and low temperature on cellular uptake*

FCM was used to investigate whether the cellular uptake of micelles was energy-dependent. Firstly, MGC80-3 cells were seeded into 6-well plates at a density of 3.0×10^5 cells/well. After incubation of 30 min at 4 °C, drug-loaded micelles (DOX concentration of 5.0 μg/ml) were added into the cells for further 1 h incubation. Then the cells were dispersed with 500 μl PBS and measured by FCM. In the control group, the treatment methods were the same except that the incubated environment was placed to 37 °C, and the uptake of the control group was set to 100%.

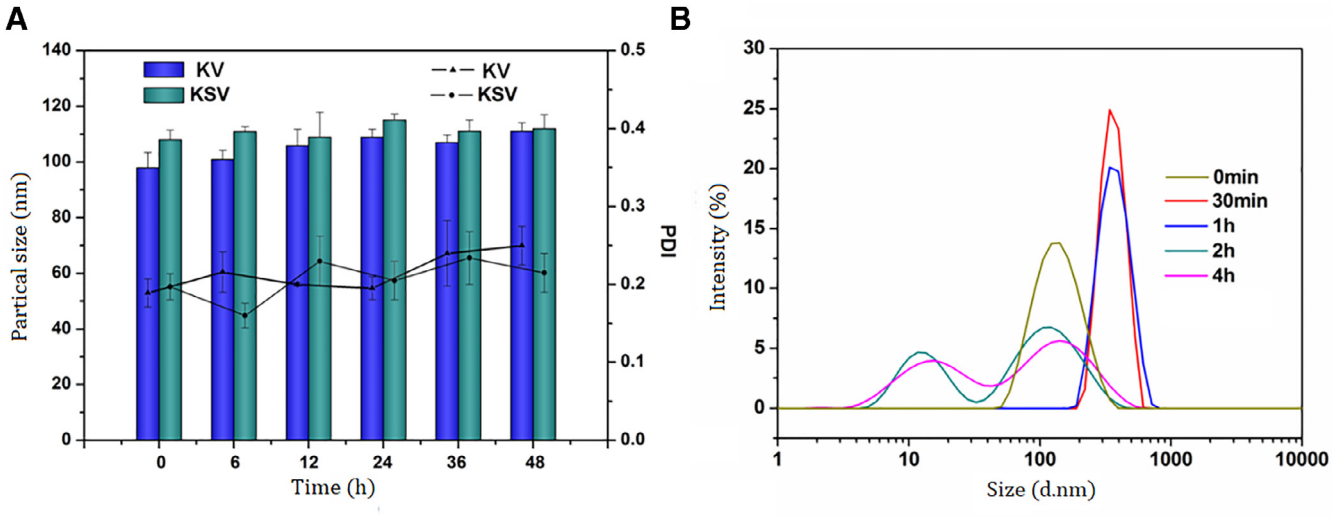

Fig. 3 – (A) Serum stability of KV and KSV micelles in DMEM containing 10% FBS. Data were presented as mean ± SD (n = 3). (B) Particle sizes distribution of KSV micelles in PBS solution (10 mM GSH, pH7.4) at 0 min, 30 min, 1 h, 2 h and 4 h.

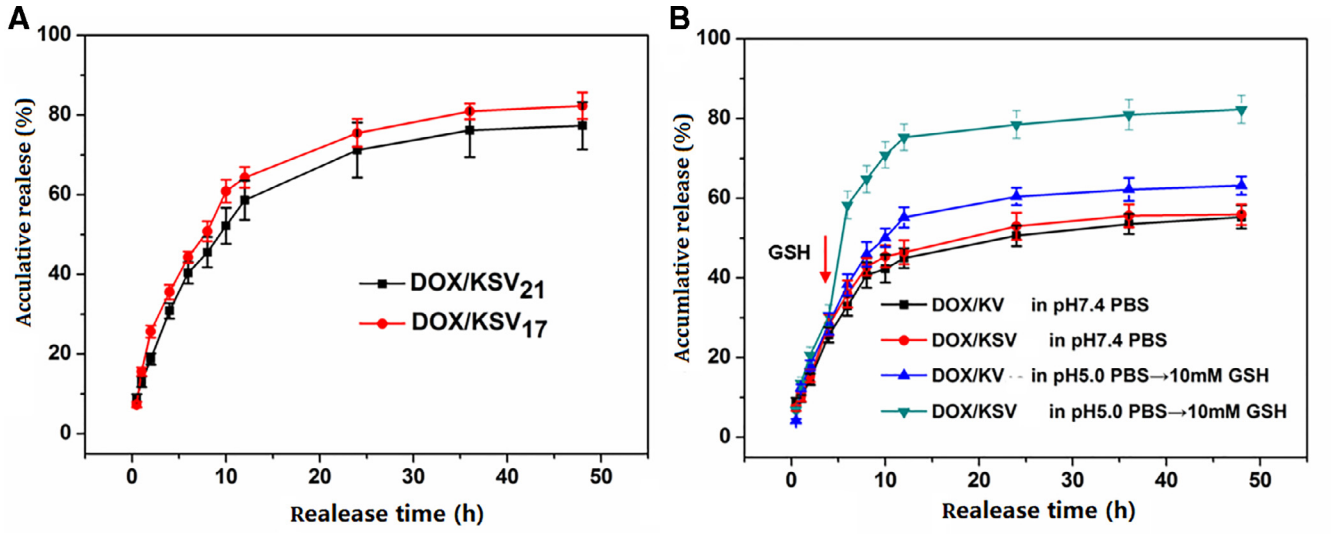

Fig. 4 – (A) *In vitro* redox-dependent release behavior of DOX/KSV micelles in GSH-containing PBS solution (10 mM, pH 5.0). (B) *In vitro* redox-dependent release behavior of drug-loaded micelles in pH 7.4 PBS and pH 5.0 PBS with 10 mM GSH at 6 h. Data were presented as mean ± standard deviation (n = 3).

2.13.2. Effects of endocytosis inhibitors on cellular uptake

The cytotoxicity of each inhibitor to MGC80-3 cells at the experimental concentration was determined by MTT assay firstly. MGC80-3 cells were seeded into 96-well plates at a density of 5×10^3 cells/well for incubation of 24 h. And then uptake inhibitors were added with the experimental concentration: quercetin (10 μg/ml) [49], chlorpromazine (10 μg/ml) [50], colchicine (40 μg/ml) [51] and indomethacin (10 μg/ml) [52] were co-incubated with MGC80-3 cells for 2 h.

Then, the uptake pathway of drug-loaded micelles was studied by FCM. MGC80-3 cells were seeded into 6-well plates at a density of 3×10^5 cells/well. The inhibitors were added to replace the old medium, and drug-loaded micelles (DOX concentration of 5 μg/ml) were incubated for 1 h and measured by flow cytometry. Cells treated with no inhibitor were used as controls and the fluorescence intensity was set to 100%.

2.14. Statistical analysis

The results were expressed as the mean ± standard deviation (SD), and all experiments were repeated at least three times independently. The unpaired students' test was adopted to determine the statistical significance of differences, $P < 0.05$.

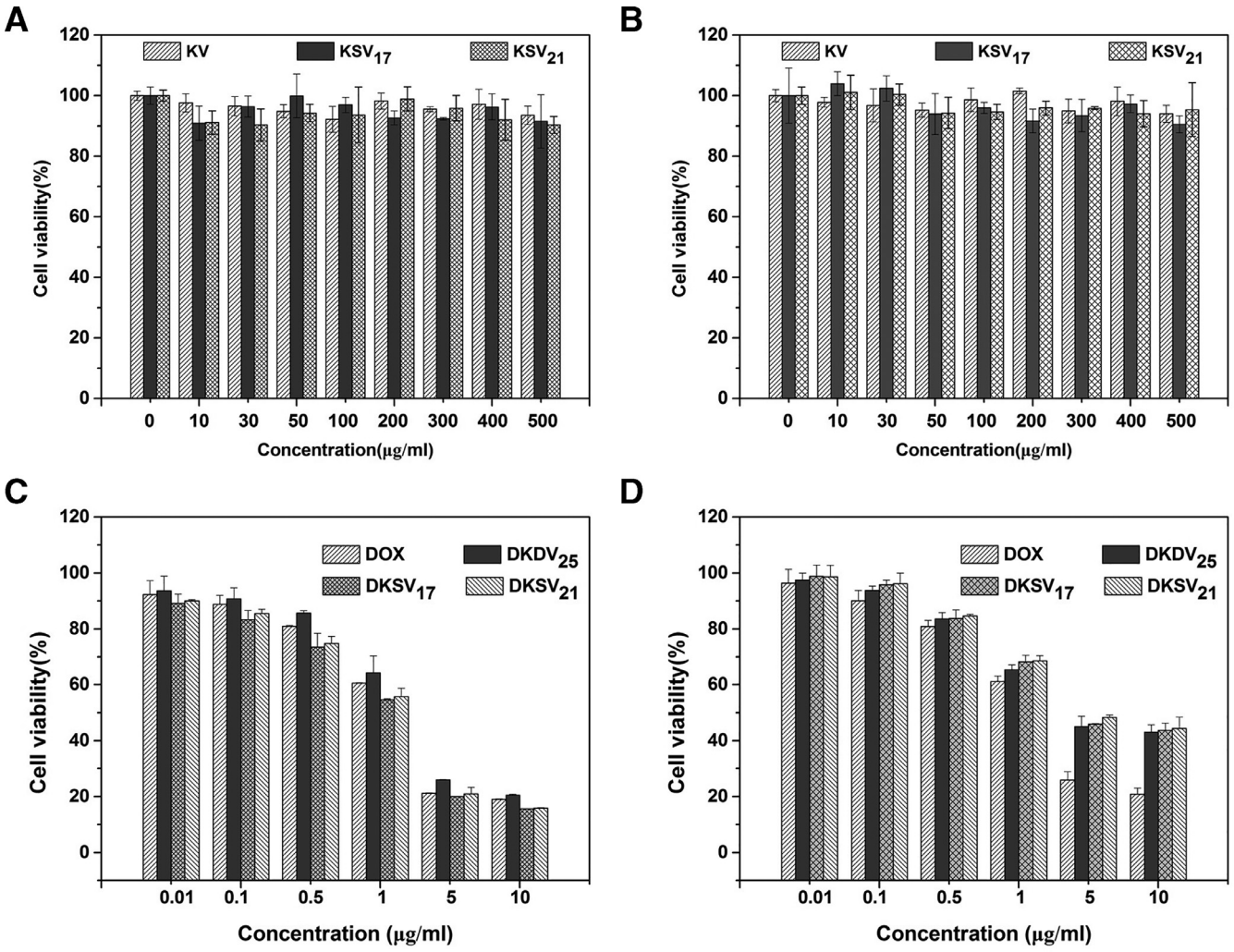

Fig. 5 – Cytotoxicity of blank micelles in (A) MGC80-3 cells and (B) COS7 cells. Cytotoxicity of DOX, DOX/KV and DOX/KSV at various DOX concentrations against (C) MGC80-3 and (D) COS7 cells after incubation for 48 h. Data were presented as mean ± standard deviation (n = 3).

3. Results and discussion

3.1. *Synthesis of redox-sensitive amphiphilic copolymer KSV*

The ^{1}H NMR spectrum of KSV is shown in Fig. 1. The carboxyl groups in heparosan polysaccharide and VES were conjugated to the -NH_2 groups of CYS, respectively. The typical peaks of glucosamine on heparosan polysaccharide were shown at 3.63 ppm, 3.83 ppm, and 5.31 ppm and the typical peak of glucosamine methylation on heparosan polysaccharide (-CO–CH_3) was shown at 1.98 ppm. The typical peaks of glucuronic acid on heparosan polysaccharide were shown at 3.29 ppm, 3.72 ppm, and 4.54 ppm. The typical peaks of methylene (-CH_2-) on the alkanes of VES were shown at 1.05–1.35 ppm and 2.85 ppm, and methyl group (-CH_3) on the phenyl ring was shown at 2.63 ppm. The typical peaks of the amide group (-CONH-) were shown between 8.05 and 8.11 ppm. Based on these results, it can be confirmed that the amphiphilic copolymer KSV has been successfully synthesized.

2.63 ppm is the typical peak of VES (-CH_3), and 5.31 ppm is the typical peak of the heparosan polysaccharide. The ratio of the integral area between the peaks was used to calculate the substitution degree of VES. Two kinds of KSV copolymers with different substitution ratios were synthesized. The substitution degrees were respectively 17% and 21%, which were expressed by KSV_{17} and KSV_{21}.

3.2. *Characterization of the micelles*

The blank micelles and drug-loaded micelles were prepared by the ultrasonic method and their physicochemical properties were characterized. The results are shown in Table 1. With the increase of the substitution degree, the particle size of both micelles decreased slightly because of the compact hydrophobic core probably. However, particle sizes of the micelles were shown all below 200 nm and presented a narrow size distribution (Fig. 2A), indicating that the micelles can be easily targeted to tumor tissue by EPR effect. The zeta potential of the micelles was kept at a negative value, which could prevent the micelles from aggregation by electrostatic repulsion.

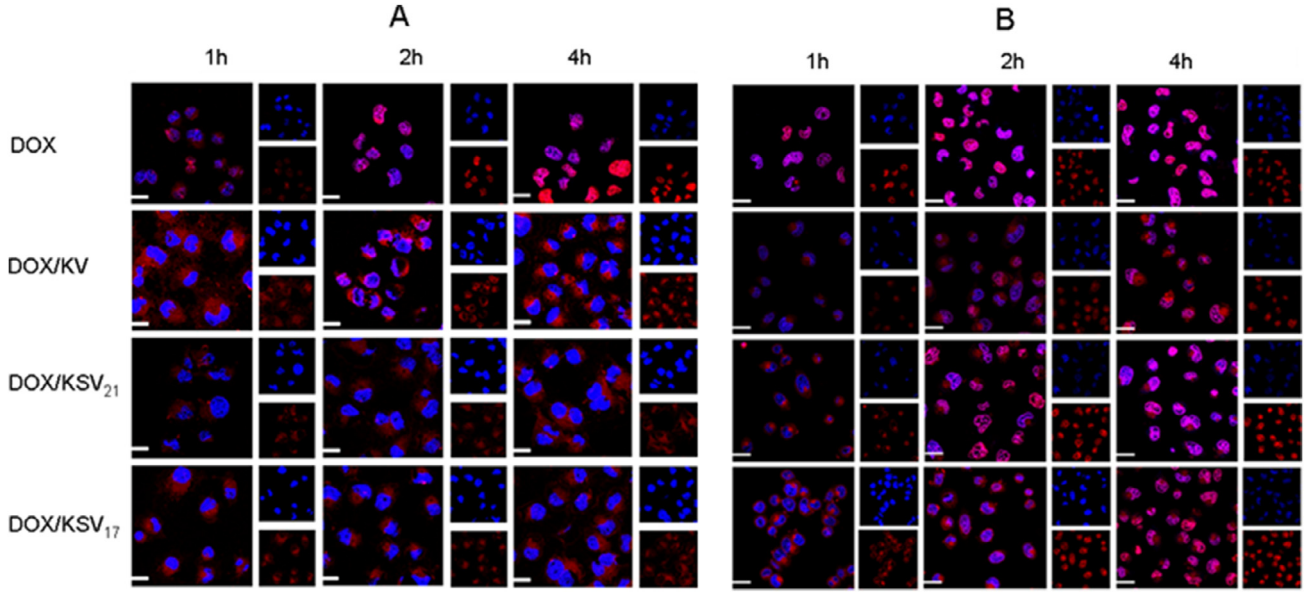

Fig. 6 – CLSM images of (A) COS7 cells and (B) MGC80-3 cells after incubation different times with DOX, DOX/KV and DOX/KSV. DOX was visualized as the red fluorescence, nucleuses labeled with Hoechst 33,342 were shown as the blue fluorescence and the merged showed purple. DOX concentration was 5 μg/ml. Scale bars correspond to 10 μm in all the images. (For interpretation of the references to colour in this figure legend, the reader is referred to the web version of this article.)

Transmission electron microscopy (TEM) (Fig. 2B) was shown that DOX/KSV had a nearly spherical morphology and good dispersibility.

As shown in Table 1, the drug loading and entrapment efficiency of the micelles were 13%–15% and 88%–90%, which means all micelles can load drug well. As the degree of substitution increased, the affinity between the hydrophobic core and the drug increased, so the drug loading and entrapment efficiency of DOX/KSV_{21} were slightly greater. Furthermore, the copolymers had small CMC values, which indicate that the micelles have better thermodynamic stability [53] and can exist stably *in vivo*.

3.3. *Serum stability and redox-sensitive of KSV*

Studies have shown that nanoparticle with high polymer content may cause blood coagulation or gelation *in vivo* [54], so it is necessary to investigate the stability of nanoparticle in serum (FBS) at 37 °C. The average size of the protein in FBS was 10 nm, which did not affect the measurement of the micelle particle size. As shown in Fig. 3A, after incubation of 48 h in FBS, no precipitates and visible particles were found, and there was no significant increase in the micellar particle size. The result indicates that only a small amount of serum proteins were adsorbed on the micelles and the micelles will not aggregate into larger particles by absorbing serum proteins after intravenous injection. Therefore, the copolymer micelles are relatively stable in serum probably due to the generation of a hydrophilic shell.

The disulfide bond in KSV structure makes it have the characteristic of redox-sensitive. In order to determine the redox-sensitive of micelles, the particle size of KSV micelles incubated with PBS solution (10 mM GSH, pH7.4) was measured by dynamic light scattering (DLS) method (Fig. 3B). It can be seen that the micelles had a good particle size at the beginning. However, the particle size was gradually increased with time extension, indicating the micelles could be disassembled and had obvious redox-sensitive property.

3.4. *In vitro redox-sensitive drug release studies*

In order to study *in vitro* release behavior of DOX/KSV and DOX/KV, pH 7.4 PBS, pH 5.0 PBS and GSH-containing PBS (10 mM, pH 5.0) were used to simulate the normal physiologic environment, tumor acid environment, and tumor intracellular redox-environment. As shown in Fig. 4A, the cumulative release of DOX from both of DOX/KSV micelles in GSH (10 mM, pH 5.0 PBS) were 82.33% and 77.34%, respectively. This indicates that the anticancer drug can be effectively released from the micelles in the tumor cell environment. It is worth noting that the cumulative release of DOX/KSV_{17} is slightly higher than that of DOX/KSV_{21} ($P < 0.05$). This may be due to the fact that DOX/KSV_{17} was disassembled faster in the reducing condition.

In addition, further experiments were designed to investigate the effect of GSH on DOX/KSV and DOX/KV micelles. As shown in Fig. 4B, the release amount of DOX/KSV and DOX/KV in pH 5.0 was higher than that at pH 7.4 ($P < 0.01$). This difference was probably due to the better solubility of DOX at low pH. However, when GSH was added at 6 h, a sudden release of DOX/KSV was observed while there was no significant change in the DOX/KV release. This also indicates that the micellar structure of DOX/KSV was disassembled in the presence of GSH resulting in the fast release of the drug. The above results indicate that DOX/KSV has stable in normal physiological condition but the drug can be released rapidly after arrival

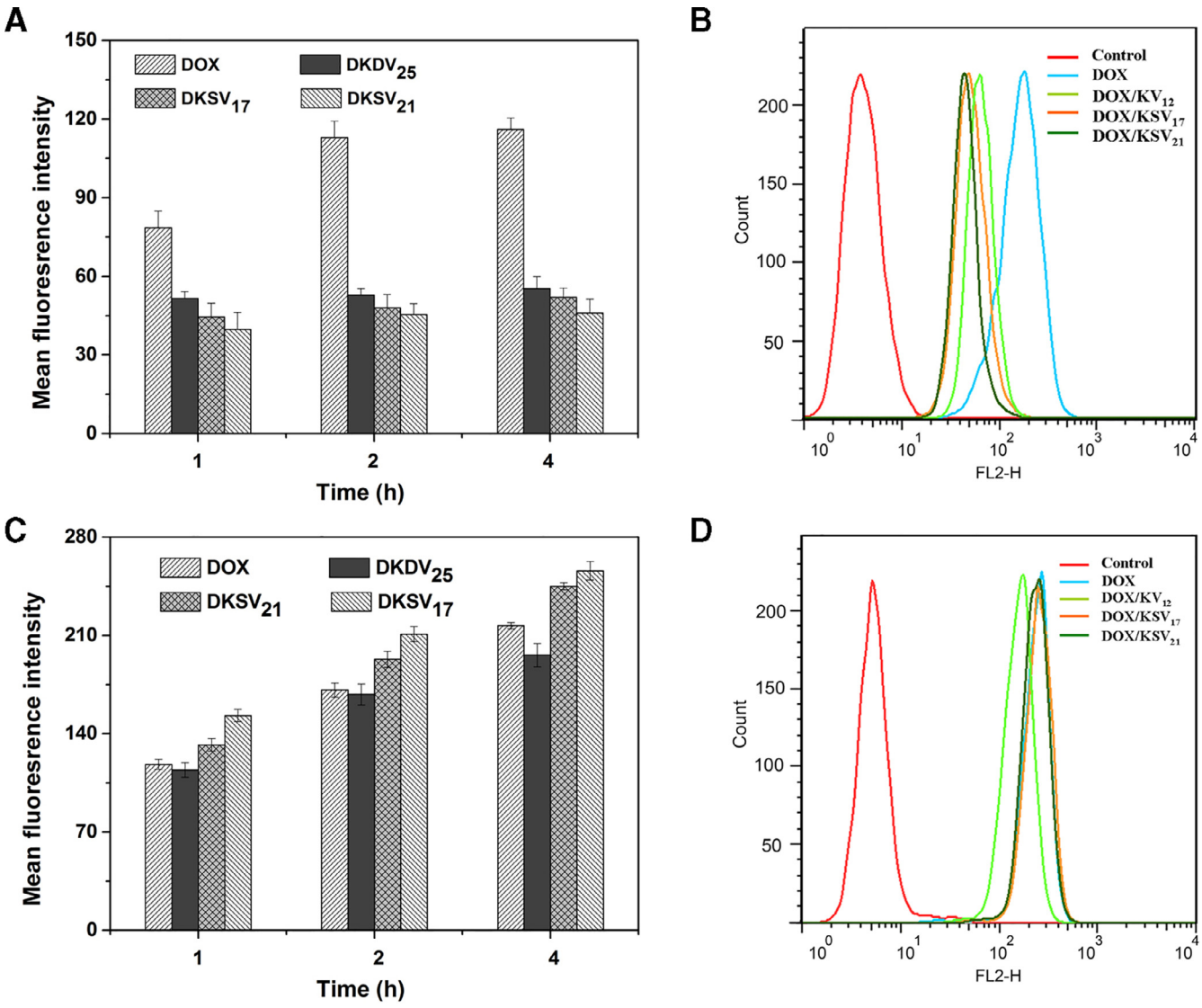

Fig. 7 – (A) Mean fluorescence intensities and (B) flow cytometry analysis profiles of different formulations in COS7 cells. (C) Mean fluorescence intensities and (D) flow cytometry analysis profiles of different formulations in MGC80-3 cells. All data were presented as mean ± SD (n = 3). DOX concentration was 5 μg/ml.

at tumor cells resulting in enhancing the efficacy of anticancer drugs.

3.5. *In vitro cytotoxicity assay*

The MTT assay was used to assess the biocompatibility of the blank micelles. The cell viability of MGC80-3 cells (Fig. 5A) and COS7 (Fig. 5B) cells were exceeded 90% even at high concentrations (500 μg/ml), suggesting the blank micelles were virtually non-toxic. The cytotoxicity of DOX/KSV and DOX/KV against MGC80-3 cells and COS7 cells is also studied (Fig. 5). As the concentration of DOX increased, both cell viabilities gradually decreased, indicating that the cytotoxicity is concentration-dependent for drug-loaded micelles. For COS7 cells, the median inhibitory concentrations (IC_{50}) of free DOX, DOX/KSV_{17}, DOX/KSV_{21} and DOX/KV were 1.752 ± 0.134, 4.931 ± 0.1622, 5.386 ± 0.209 and 4.717 ± 0.211 μg/ml respectively. There was a significant difference between free DOX and micelles ($P < 0.001$), but the cytotoxicity of all the micelle groups was similar. Because the level of GSH was low in normal cells, the release rate of DOX from DOX/KSV was slow resulting in no significant difference in the IC_{50} values of DOX/KSV and DOX/KV micelles. However, in MGC80-3 cells, the IC_{50} value of DOX/KSV (1.003 ± 0.067 μg/ml) was significantly lower than that of DOX/KV(4.717 ± 0.211 μg/ml). This could be attributed to the rapid release of DOX from DOX/KSV resulting from the high concentration of GSH in tumor cells. It was worth noting that the IC_{50} value of DOX/KSV micelles against MGC80-3 cells was about 5-fold higher than that of COS7 cells ($P < 0.001$), indicating that redox-sensitive micelles have better selectivity for tumor cells.

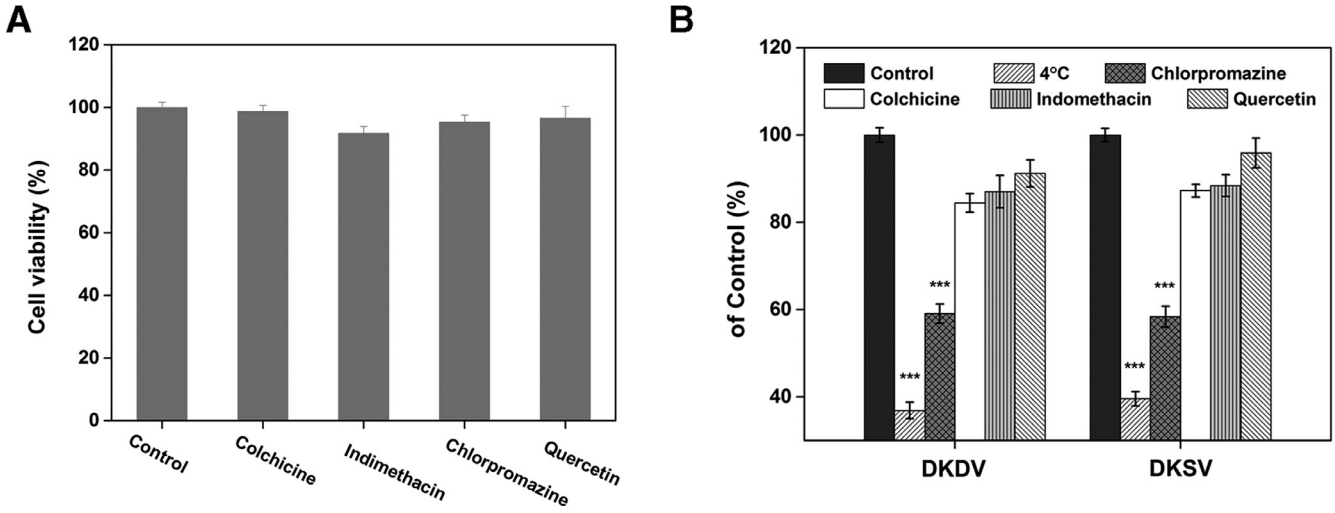

Fig. 8 – (A) Cytotoxicity of the endocytosis inhibitors at the chosen concentration against MGC80-3 cells. (B) Effects of low temperature and endocytosis inhibitors on uptake of DOX/KSV and DOX/KV in MGC80-3 cells. Data were presented as mean ± standard deviation (n = 3). * indicated $P < 0.001$.**

3.6. *Cellular uptake study*

CLSM was used to qualitatively investigate the *in vitro* cellular uptake of DOX/KSV and DOX/KV in MGC80-3 cells and COS7 cells. After co-incubated with free DOX, DOX/KSV_{17}, DOX/KSV_{21} and DOX/KV micelles, MGC80-3 cells and COS7 cells were observed by CLSM. As shown in Fig. 6, DOX was mainly concentrated in the cytoplasm after incubation for 1 h, but more drugs were entered into the nucleus in free DOX group. For all groups, the fluorescence intensity of DOX increased after co-incubated for 2 h and 4 h. It was worth noting that most of DOX in the micelle groups remained in the cytoplasm after co-incubation for 4 h in COS7 cells (Fig. 6A), which indicated that the drugs were not released quickly from the micelles. However, in MGC80-3 cells (Fig. 6B), DOX was released gradually from the drug-loaded micelles into the nucleus after co-incubated for 2 h. And it was not difficult to see that DOX/KSV disassembled faster and had stronger fluorescence signal than DOX/KV, which also was caused by the redox-sensitive behavior of micelles.

FCM was used to further quantitatively test the cellular uptake of DOX/KSV and DOX/KV in tumor and normal cells. In COS7 cells, there was no significant difference in the mean fluorescence intensities of DOX/KSV and DOX/ KV (Fig. 7A and B). However, the cellular uptake of redox-sensitive micelles was significantly higher than that of redox-insensitive micelles ($P < 0.001$) in MGC80-3 cells (Fig. 7C and 7D). The results indicate that redox-sensitive DOX/KSV micelles can be more uptaken by tumor cells.

3.7. *Study of the endocytosis pathways*

In order to determine the potential endocytic pathway of micelles, a series of uptake inhibitors were used. Specifically, chlorpromazine is an inhibitor of clathrin-mediated endocytosis, indomethacin is an inhibitor of caveolae-mediated endocytosis, colchicine is an inhibitor of macropinocytosis, and quercetin is an inhibitor of clathrin/caveolae-independent endocytosis. Fig. 8A clearly shows the cytotoxicity of each inhibitor to MGC80-3 cells, which indicates that the inhibitor had no toxicity with cell viability above 90% at the experimental concentration. Therefore, cellular uptake inhibition was not caused by inhibitor toxicity. Then the uptake of micelles in MGC80-3 cells after treatment with different inhibitors is shown in Fig. 8B. Compared to the control, a significant reduction was observed at low temperatures and the uptake rates of DOX/KV and DOX/KSV decreased to 36.89% and 39.59% ($P < 0.001$), respectively (Fig. 8), which indicates that the uptake pathway of the micelles is an energy-dependent pathway. In addition, the uptake of DOX/KV and DOX/KSV micelles decreased to 59.07% ($P < 0.001$) and 58.37% ($P < 0.001$), respectively in presence of chlorpromazine. And after DOX/KV and DOX/KSV treated with colchicine and indomethacin, the uptake was decreased to 84.46%, 87.04% ($P < 0.05$) and 87.24%, 88.41%, ($P < 0.05$) respectively. However, there was no significant change after treatment with quercetin. These results indicate that though clathrin- and caveolae-mediated endocytosis both affect cellular uptake of the heparosan-based micelle, clathrin-mediated endocytosis plays a major role.

4. Conclusion

In this study, the redox-sensitive heparosan-based amphiphilic copolymers were designed and they self-assembled into micelles in aqueous solution. The DOX/KSV micelles could remain stable under plasma and physiological conditions but dissociate and release DOX in the tumor microenvironment. So DOX/KSV had reduction sensitivity and could be internalized in tumor cells to release more anticancer drugs rapidly. The cytotoxicity of drug-loaded micelles in tumor cells was significantly higher than that of normal cells,

and the redox-sensitive micelles DOX/KSV had more toxicity than redox-insensitive micelles DOX/KV in MGC80-3 cells. Moreover, drug-loaded micelles could enter cancer cells more efficiently compared with normal cells, and DOX/KSV disassembled rapidly in tumor cells to release DOX. In addition, a low degree of KSV micelles showed a better antitumor activity. The micelles were uptaken into tumor cells via multiple pathways and primarily through clathrin-mediated endocytosis. Therefore, redox-sensitive DOX/KSV micelles can effectively deliver antitumor drugs to tumors while reducing side effects on normal tissues and heparosan-based polymers have great potential as effective drug carriers.

Declaration of interest

The authors report no conflicts of interest. The authors alone are responsible for the content and writing of this article.

Acknowledgments

We are grateful for the financial support from National Natural Science Foundation of China (81503007 and 21574059), Research Project of Wuxi Health and Family Planning Commission (Q201843), Natural Science Foundation of Jiangsu Province (BK20170202) and the Top-notch Academic Programs Project of Jiangsu Higher Education Institutions (PPZY2015B146).

REFERENCES

[1] Ha W, Zhao XB, Chen XY, Jiang K, Shi YP. Prodrug-based cascade self-assembly strategy for precisely controlled combination drug therapy. ACS Appl Mater Interfaces 2018;10(25):21149–59.
[2] Zhu C, Huo D, Chen Q, Xue J, Shen S, Xia Y. A eutectic mixture of natural fatty acids can serve as the gating material for near-infrared-triggered drug release. Adv Mater 2017;29(40):1703702.
[3] Zhang LH, Qin Y, Zhang ZM, Fan F, Huang C, Lu L, et al. Dual pH/reduction-responsive hybrid polymeric micelles for targeted chemo-photothermal combination therapy. Acta Biomater 2018;75(18):371–85.
[4] Cho HJ, Yoon IS, Hong YY, Koo H, Jin YJ, Ko SH, et al. Polyethylene glycol-conjugated hyaluronic acid-ceramide self-assembledNanoparticles for targeted delivery of doxorubicin. Biomaterials 2012;33(4):1190–200.
[5] Jia N, Ye Y, Wang Q, Zhao X, Hu H, Chen D, et al. Preparation and evaluation of poly (L-histidine) based pH-sensitive micelles for intracellular delivery of doxorubicin against MCF-7/ADR cells. Asian J Pharm Sci 2017;12(5):433–41.
[6] Li Z, Tao W, Zhang D, Wu C, Song B, Wang S, et al. The studies of PLGA nanoparticles loading atorvastatin calcium for oral administration *in vitro* and *in vivo*. Asian J Pharm Sci 2016;12(3):285–91.
[7] Danhier F, Feron O, Préat V. To exploit the tumor microenvironment: Passive and active tumor targeting of nanocarriers for anti-cancer drug delivery. J Controlled Release 2010;148(2):135–46.
[8] Kim D, Zhong Gao ZG, Lee ES, Bae YH. *In vivo* evaluation of doxorubicin-loaded polymeric micelles targeting folate receptors and early endosomal pH in drug-resistant ovarian cancer. Mol Pharm 2009;6(5):1353–62.
[9] Daglar B, Ozgur E, Corman ME, Uzun L, Demirel GB. Polymeric nanocarriers for expected nanomedicine: current challenges and future prospects. RSC Advance 2014;4(89):639–59.
[10] Zhang X, Li L, Li C, Hua Z, Song H, Xiong F, et al. Cisplatin-crosslinked glutathione-sensitive micelles loaded with doxorubicin for combination and targeted therapy of tumors. Carbohydr Polym 2017;155:407–15.
[11] Zhong Y, Goltsche K, Cheng L, Xie F, Meng F, Deng C, et al. Hyaluronic acid-shelled acid-activatable paclitaxel prodrug micelles effectively target and treat CD44-overexpressing human breast tumor xenografts *in vivo*. Biomaterials 2016;84:250–61.
[12] Gong J, Chen M, Zheng Y, Wang S, Wang Y. Polymeric micelles drug delivery system in oncology. J Control Release 2012;159(3):312–23.
[13] Ma N, Li Y, Xu H, Wang Z, Zhang X. Dual redox responsive assemblies formed from diselenide block copolymers. J Am Chem Soc 2010;132(2):442–3.
[14] Kedar U, Phutance P, Shidhaye S, Kadam V. Advances in polymeric micelles for drug delivery and tumor targeting. Nanomedicine 2010;6(6):714–29.
[15] Li J, Yin T, Wang L, Yin L, Zhou J, Huo M. Biological evaluation of redox-sensitive micelles based on hyaluronic acid-deoxycholic acid conjugates for tumor-specific delivery of paclitaxel. Int J Pharm 2015;483(1–2):38–48.
[16] Jiang X, Li L, Liu J, Hennink WE, Zhuo R. Facile fabrication of thermo-responsive and reduction-sensitive polymeric micelles for anticancer drug delivery. Macromol Biosci 2012;12(5):703–11.
[17] Zeng L, Li Y, Li T, Cao W, Yi Y, Geng W, et al. Selenium-platinum coordination compounds as novel anticancer drugs: selectively killing cancer cells via a reactive oxygen species (ROS)-mediated apoptosis route. Chem Asian J 2014;9(8):2295–302.
[18] Lili Y, Ruihua M, Li L, Fei L, Lin Y, Li S. Intracellular doxorubicin delivery of a core cross-linked, redox-responsive polymeric micelles. Int J Pharm 2016;498(1-2):195–204.
[19] Yang Q, Tan L, He C, Liu B, Xu Y, Zhu Z. Redox-responsive micelles self-assembled from dynamic covalent block copolymers for intracellular drug delivery. Acta Biomaterialia 2015;17:193–200.
[20] Siegwart DJ, Whitehead KA, Nuhn L, Sahay G, Cheng H, Jiang S, et al. Combinatorial synthesis of chemically diverse core-shell nanoparticles for intracellular delivery. Proc Natl Acad Sci USA 2011;108(32):12996–3001.
[21] Miteva M, Kirkbride KC, Kilchrist KV, Werfel TA, Li H, Nelson CE, et al. Tuning PEGylation of mixed micelles to overcome intracellular and systemic sirna delivery barriers. Biomaterials 2015;38:97–107.
[22] Hatakeyama H, Akita H, Harashima H. A multifunctional envelope type nano device (MEND) for gene delivery to tumours based on the EPR effect: A strategy for overcoming the PEG dilemma. Adv Drug Deliv Rev 2011;63(3):152–60.
[23] Holland JW, Hui C, Cullis PR, Madden TD. Poly(ethylene glycol)−lipid conjugates regulate the calcium-induced fusion of liposomes composed of phosphatidylethanolamine and phosphatidylserine. Biochemistry 1996;35(8):2618–24.
[24] Kim JH, Kim YS, Park K, Kang E, Lee S, Nam HY, et al. Self-assembled glycol chitosan nanoparticles for the sustained and prolonged delivery of antiangiogenic small peptide drugs in cancer therapy. Biomaterials 2008;29(12):1920–30.
[25] Coradini D, Pellizzaro C, Scarlata I, Zorzet S, Garrovo C, Abolafio A, et al. Novel retinoic/butyric hyaluronan ester for the treatment of acute promyelocytic leukemia: preliminary preclinical results. Leukemia 2006;20(5):785–92.

[26] Park K, Kim K, Kwon IC, Kim SK, Lee S, Lee DY, et al. Preparation and characterization of self-assembled nanoparticles of heparin-deoxycholic acid conjugates. Langmuir 2004;20(26):11726–31.
[27] Deangelis PL. HEPtune: A process of conjugating a naturally occurring sugar molecule, heparosan, to a drug for enhanced drug delivery. Drug Deliv 2013;3(1):1–5.
[28] Jing W, Roberts JW, Green DE, Almond A, Deangelis PL. Synthesis and characterization of heparosan-granulocyte-colony stimulating factor conjugates: a natural sugar-based drug delivery system to treat neutropenia. Glycobiology 2017;27(11):1052–61.
[29] Hubbell JA, Chilkoti A. Nanomaterials for drug delivery. Science 2012;337(6092):303–5.
[30] Guo X, Shi C, Wang J, Di S, Zhou S. pH-triggered intracellular release from actively targeting polymer micelles. Biomaterials 2013;34(18):4544–54.
[31] Gao Y, Chen Y, Ji X, He X, Yin Q, Zhang Z, et al. Controlled intracellular release of doxorubicin in multidrug-resistant cancer cells by tuning the shell-pore sizes of mesoporous silica nanoparticles. ACS Nano 2011;5(12):9788–98.
[32] Woraphatphadung T, Sajomsang W, Gonil P, Saesoo S, Opanasopit P. Synthesis and characterization of pH-responsive N-naphthyl-N,O-succinyl chitosan micelles for oral meloxicam delivery. Carbohydr Polym 2015;121:99–106.
[33] Yuan W, Zou H, Shen J. Amphiphilic graft copolymers with ethyl cellulose backbone: Synthesis, self-assembly and tunable temperature-CO_2 response. Carbohydr Polym 2016;136:216–23.
[34] Naeem M, Yoo JW. Withdrawn: Budesonide-loaded enzyme- and pH-sensitive polymeric nanoparticles for the treatment of colitis. Asian J Pharm Sci 2015;430:463–7.
[35] Zhao YP, Ye WL, Liu DZ, Cui H, Cheng Y, Liu M, et al. Redox and pH dual sensitive bone targeting nanoparticles to treat breast cancer bone metastases and inhibit bone resorption. Nanoscale 2017;9(19):6264–77.
[36] Wang JX, Yang XZ. Near infrared light-activated super-sensitive drug release using nanoparticles with a flow core. J Controlled Release 2017;259:145.
[37] Anirudhan TS, Christa J, Binusreejiayan. pH and magnetic field sensitive folic acid conjugated protein–polyelectrolyte complex for the controlled and targeted delivery of 5-fluorouracil. J Ind Engin Chem 2018;57:199–207.
[38] Papa AL, Korin N, Kanapathipillai M, Mammoto A, Mammoto T, Jiang A, et al. Ultrasound-sensitive nanoparticle aggregates for targeted drug delivery. Biomaterials 2017;139:187–94.
[39] Nguyen Thi TT, Tran TV, Tran NQ, Nguyen CK, Nguyen DH. Hierarchical self-assembly of heparin-PEG end-capped porous silica as a redox sensitive nanocarrier for doxorubicin delivery. Mater Sci Eng C Mater Biol Appl 2017;70(Pt 2):947–54.
[40] Zhai S, Hu X, Hu Y, Wu B, Xing D. Visible light-induced crosslinking and physiological stabilization of diselenide-rich nanoparticles for redox-responsive drug release and combination chemotherapy. Biomaterials 2017;121:41–54.
[41] Yu LL Y, Mu RH, Li L, Liang F, Yao L, Su L. Intracellular doxorubicin delivery of a core cross-linked, redox-responsive polymeric micelles. Int J Pharm 2016;498(1-2):195–204.
[42] Yang Q, Tan L, He C, Liu B, Xu Y, Zhu Z, et al. Redox-responsive micelles self-assembled from dynamic covalent block copolymers for intracellular drug delivery. Acta Biomater 2015;17:193–200.
[43] Lin JT, Liu ZK, Zhu QL, Rong XH, Liang CL, Wang J, et al. Redox-responsive nanocarriers for drug and gene co-delivery based on chitosan derivatives modified mesoporous silica nanoparticles. Colloids Surf B Biointerfaces 2017;155:41–50.
[44] Yang HY, Jang MS, Li Y, Lee JH, Lee DS. Multifunctional and redox-responsive self-assembled magnetic nanovectors for protein delivery and dual-modal imaging. ACS Appl Mater Interfaces 2017;9(22):184–92.
[45] Liu L, Yi H, He H, Pan H, Cai L, Ma Y. Tumor associated macrophage-targeted microRNA delivery with dual-responsive polypeptide nanovectors for anti-cancer therapy. Biomaterials 2017;134:166–79.
[46] Wen H, Dong H, Liu J, Shen A, Li Y, Shi DL. Redox-mediated dissociation of PEG–polypeptide-based micelles for on-demand release of anticancer drugs. J Mater Chem B 2016;4(48):7859–69.
[47] Choi WI, Yoon KC, Im SK, Kim YH, Yuk SH, Tae G. Remarkably enhanced stability and function of core/shell nanoparticles composed of a lecithin core and a pluronic shell layer by photo-crosslinking the shell layer: *In vitro* and *in vivo* study. Acta Biomater 2010;6(7):2666–73.
[48] Liu C, Yuan J, Luo X, Chen M, Chen Z, Zhao Y, et al. Folate-decorated and reduction-sensitive micelles assembled from amphiphilic polymer-camptothecin conjugates for intracellular drug delivery. Mol Pharm 2014;11(11):4258–69.
[49] Sahay G, Alakhova DY, Kabanov AV. Endocytosis of nanomedicines. J Control Release 2010;145(3):182–95.
[50] Gersdorff KV, Sanders NN, Vandenbroucke R, Smedt SCD, Wagner E, Ogris M. The internalization route resulting in successful gene expression depends on both cell line and polyethylenimine polyplex type. Mol Ther 2006;14(5):745–53.
[51] Cheng L, Huang FZ, Cheng LF, Zhu YQ, Hu Q, Li L, et al. GE11-modified liposomes for non-small cell lung cancer targeting: preparation, *ex vitro* and *in vivo* evaluation. Int J Nanomedicine 2014;9:921–35.
[52] Manunta M, Tan PH, Sagoo P, Kashefi K, George AJ. Gene delivery by dendrimers operates via a cholesterol dependent pathway. Nucleic Acids Res 2004;32(9):2730–9.
[53] Du JZ, Tang LY, Song WJ, Shi Y, Wang J. Evaluation of polymeric micelles from brush polymer with poly(epsilon-caprolactone)-b-poly(ethylene glycol) side chains as drug carrier. Biomacromolecules 2009;10(8):2169–74.
[54] Verma A, Stellacci F. Effect of surface properties on nanoparticle-cell interactions. Small 2010;6(1):12–21.